

Radical Ion Salts of 2,3-Dichloro-5,6-dicyanobenzoquinone and Metallocenes. A Reexamination of Their Magnetic and Spectroscopic Properties

Joel S. Miller,^{*†} Paul J. Krusic,[†] David A. Dixon,[†] William Michael Reiff,^{*‡}
Jian H. Zhang,[†] Eric C. Anderson,[§] and Arthur J. Epstein[§]

Contribution No. 3884 from the Central Research and Development Department, E. I. du Pont de Nemours & Co., Inc., Wilmington, Delaware 19898, Department of Chemistry, Northeastern University, Boston, Massachusetts 02115, and the Departments of Physics and Chemistry, The Ohio State University, Columbus, Ohio 43210-1106. Received November 14, 1985

Abstract: On the basis of UV-vis, infrared, and Mössbauer spectroscopies and electron spin resonance we have established that the anion of the salts formed from 2,3-dichloro-5,6-dicyanobenzoquinone (DDQ) and cobaltocene or decamethylferrocene is not the benzohydroquinone anion, [DDQH]⁻, as previously postulated, but rather the [DDQ]^{•-} radical anion. A full $S = 1/2$ spin/DDQ ($g = 2.00517$, $a_{14} = 0.59$, $a_{13} = 4.72$, 4.31 , and 2.78 G) is observed by ESR for [Co(C₅H₅)₂][DDQ] in solution, whereas as previously reported it possesses <1% $S = 1/2$ spin/DDQ in the solid state. As the temperature is increased the ESR of the solid signal increases and the behavior is fit to a singlet-triplet behavior ($E_a \sim 0.25$ eV). To account for this a structure based on a weak [DDQ]₂²⁻ dimer, as reported, for example, for [NET₄][DDQ], is proposed. In contrast, a full $S = 1/2$ spin/DDQ is observed for [Co(C₅Me₅)₂][DDQ] in either solution or the solid. The magnetic susceptibility characterizes this latter compound as Curie-like for $T > 2$ K. The [DDQ]^{•-} exhibits several characteristic spectroscopic signatures [IR: $\nu_{\text{CN}} = 2220$ cm⁻¹ (s) and $\nu_{\text{C}=\text{O}} = 1580$ cm⁻¹ [the 1670 cm⁻¹ ν_{CO} absorption present in DDQ is absent]; UV-vis: λ_{max} with $\epsilon > 4000$ M⁻¹ cm⁻¹ are found at 17 000, 18 300, 19 700, 21 900, 23 150, 28 800, 37 000, 38 900, and 40 500 cm⁻¹. The $S = 1/2$ [DDQ]^{•-} in the [Co(C₅Me₅)₂]⁺ salt is monomeric as the complex is isostructural to [Fe(C₅Me₅)₂]⁺[DDQ]^{•-}. Ab initio molecular orbital calculations on DDQ and [DDQ]^{•-} are in good agreement with the observed structural, ESR, and UV-vis data. The [DDQ]^{•-} is stable in solution, and the absorptions in the 18 000–25 000 cm⁻¹ region are assigned to the first internal transition ($2A_2 \leftarrow 2B_1$). The calculated spin and charge densities for [DDQ]^{•-} show that the majority of the charge resides on the N, O, and Cl, while the majority of the spin resides on the C=O and C≡N $p\pi$ orbitals.

We have investigated the nature of the 2,3-dichloro-5,6-dicyano-*p*-benzoquinone, DDQ, species in a number of metallocene complexes. The anion formed by electron transfer from the metallocene has been postulated by Hendrickson and co-workers and by us to be present as the diamagnetic hydroquinone anion, [DDQH]⁻. We find that the anion should be described as the radical anion, [DDQ]^{•-}. Brandon et al.¹ first synthesized the DDQ complexes of ferrocene and cobaltocene and formulated the anion as [DDQ]^{•-}. Likewise, [DDQ]^{•-} was reported by Ichikawa et al.^{2a} and Omote et al.^{2b} to be the counterion of biferrocenium complexes. Hendrickson and co-workers³ reinvestigated the biferrocene oxidation by DDQ and instead proposed that the anion is [DDQH]⁻. The diamagnetic [DDQH]⁻ anion was postulated by investigating the DDQ salt of cobaltocene and reporting that although it possesses an organic free radical ESR signal, the magnetic susceptibility indicated <0.2% radical anion. Thus, the [DDQ]^{•-} radical anion formulation was discarded in favor of the diamagnetic hydroquinone, [DDQH]⁻.^{3b} Since then Hendrickson and co-workers,⁴⁻⁵ Sano and co-workers,⁶ and ourselves⁷ have accepted this formulation. Recently, in our quest to understand the metamagnetic behavior of one-dimensional [Fe(C₅Me₅)₂]⁺[TCNQ]^{•-} (1:1) (TCNQ = 7,7,8,8-tetracyano-*p*-quinodimethane), we have studied the low-temperature ⁵⁷Fe Mössbauer spectra of several [Fe(C₅Me₅)₂]⁺ salts. We report herein that the DDQ in the Co(C₅H₅)₂ and Fe(C₅Me₅)₂ salts is the $S = 1/2$ anion [DDQ]^{•-} and not the $S = 0$ [DDQH]⁻. We also present a molecular orbital study of DDQ and [DDQ]^{•-}.

Experimental Section

The DDQ salts of cobaltocene¹ and decamethylferrocene⁷ were prepared in an HE501 Vacuum Atmosphere inert atmosphere box (<1 ppm H₂O; <1 ppm O₂) by methods previously described in the literature. Decamethylcobaltocene was prepared by the literature route⁸ from [Co(C₅Me₅)₂][PF₆] (Strem). The DDQ (Aldrich) was recrystallized from chloroform prior to use. Cobaltocene (Alfa) was sublimed prior to use and Fe(C₅Me₅)₂ (Strem) was used as received. Acetonitrile was

distilled under argon twice (first from P₂O₅ and finally from CaH₂) prior to use. The hydroquinone (2,5-dichloro-5,6-dicyano-1,4-dihydroxybenzene) was prepared from DDQ by a literature procedure.⁹ Except for the sodium salts the analytically pure DDQ salts described below were prepared without special precautions to exclude oxygen or water.

Electronic absorption and vibrational spectra were recorded on Cary 2300 and Perkin Elmer 283B spectrophotometers, respectively. Temperature-dependent ESR data were recorded on a Bruker ER420 ESR spectrometer. Magnetic susceptibility was determined by the Faraday method with use of a previously described system.⁷ Elemental analysis and unit cell constant determinations were performed by Galbraith Laboratories (Knoxville, TN) and Molecular Structures, Inc. (College Station, TX). Zero-field Mössbauer spectra were determined with a conventional constant acceleration spectrometer with a source of 150 mCi ⁵⁷Co electroplated onto the surface and annealed into the body of a 6 μ m thick foil of high-purity rhodium. The details of cryogenics, temperature control, etc. have been described previously.¹⁰

Molecular orbital calculations were performed with the HONDO program¹¹ on an IBM-3081 computer. The STO-3G basis set¹² was used for these calculations since a qualitative picture of the bonding was

- (1) Brandon, R. L.; Osiecki, J. H.; Ottenberg, A. *J. Org. Chem.* **1966**, *31*, 1214-1217.
- (2) (a) Ichikawa, M.; Soma, M.; Onishi, T.; Tamaru, K. *Trans. Faraday Soc.* **1967**, *63*, 2528. (b) Omote, Y.; Komatsu, T.; Kobayashi, R.; Sugiyama, N. *Tetrahedron Lett.* **1972**, 93-96.
- (3) (a) Morrison, W. H., Jr.; Hendrickson, D. N. *Chem. Phys. Lett.* **1973**, *22*, 119-123. (b) Morrison, W. H., Jr.; Krogsrud, S.; Hendrickson, D. N. *Inorg. Chem.* **1973**, *12*, 1998-2004.
- (4) Morrison, W. H., Jr.; Hendrickson, D. N. *Inorg. Chem.* **1975**, *14*, 2331-2346.
- (5) Wollmann, R. G.; Hendrickson, D. N. *Inorg. Chem.* **1977**, *16*, 3079-3089.
- (6) Iijima, S.; Saida, R.; Motoyama, I.; Sano, H. *Bull. Chem. Soc. Jpn.* **1981**, *54*, 1375-1379.
- (7) Gebert, E.; Reis, A. H., Jr.; Miller, J. S.; Rommelmann, H.; Epstein, A. J. *J. Am. Chem. Soc.* **1982**, *104*, 4403-4410.
- (8) Robbins, J. L.; Edelstein, N.; Spencer, B.; Smart, J. C. *J. Am. Chem. Soc.* **1982**, *104*, 1882-1893.
- (9) Baride, E. A.; Brook, A. G.; Linstead, R. P. *J. Chem. Soc.* **1954**, 3569-3575.
- (10) Cheng, C.; Reiff, W. M. *Inorg. Chem.* **1977**, *16*, 2097.
- (11) (a) Dupuis, M.; Rys, J.; King, H. F. *J. Chem. Phys.* **1976**, *65*, 111. (b) King, H. F.; Dupuis, M.; Rys, J. *National Resource for Computer Chemistry Software Catalog*, Vol 1, Program QHO2 (HONDO), 1980.
- (12) Hehre, W. J.; Stewart, R. F.; Pople, J. A. *J. Chem. Phys.* **1969**, *51*, 2657.

^{*} E. I. du Pont de Nemours & Co., Inc.

[†] Northeastern University.

[§] Ohio State University.

desired. The geometries were gradient optimized.¹³ The calculations on the closed-shell DDQ were done at the RHF level while the calculations on the doublet anion [DDQ]⁻ were done at the UHF level. Although the electron is bound, the small basis set precludes an RHF open-shell calculation on [DDQ]⁻ due to convergence problems. Furthermore, the UHF form of the wave function is more useful for providing information on the spin density of [DDQ]⁻.

[Et₄N]⁺[DDQ]⁻ was prepared from [Et₄N]⁺I⁻ (347 mg; 1.351 mmol) and DDQ (205 mg; 0.903 mmol) in ca. 50 mL of acetonitrile.¹⁴ After the volume of solvent was reduced to ca. 10 mL the solution was stored at -20 °C for 14 h. Black-purple black crystals (86 mg; 0.24 mmol; 27%) were isolated upon filtration. Unit cell parameters were found to be identical with the values previously reported in the literature.^{14,15} i.e., *a* = 12.497 (3) Å, *b* = 20.101 (4) Å, *c* = 6.991 (1) Å, and β = 98.76 (1)°, *V* = 1733.19 Å³, space group = *P*₂/n (literature values: *a* = 12.493 (5) Å, *b* = 20.114 (7) Å, *c* = 6.996 (3) Å, β = 98.79 (8)°, *V* = 1737 (1) Å³, space group = *P*₂/n).

[Co(C₅Me₅)₂]⁺[DDQ]⁻ was prepared in a drybox from Co(C₅Me₅)₂ (100.0 mg; 0.3036 mmol) dissolved in 6 mL of acetonitrile and 69.0 mg of DDQ (0.3036 mmol) dissolved in 6 mL of MeCN. After the solution was left standing at room temperature, 150 mg (89%) of dark brown crystals separated and were collected by filtration. Attempts to grow larger crystals by slow cooling were not successful. The unit cell parameters of [Co(C₅Me₅)₂]⁺[DDQ]⁻ were determined by the least-squares refinement of the powder diffraction data taken on a Philips-Norelco APD-3600 diffractometer and by comparison with the powder diffraction data taken for the iron analogue where the space group and unit cell had previously been determined.⁷ The orthorhombic unit cell parameters were determined to be the following: *a* = 17.06 Å, *b* = 14.52 Å, *c* = 10.52 Å, *V* = 2603 Å³. Using the same refinement procedure, we obtain *a* = 17.05 Å, *b* = 14.89 Å, *c* = 10.71 Å, and *V* = 2719 Å³ for the iron analogue. This is in good agreement with the literature⁷ values of *a* = 17.027 Å, *b* = 14.497 Å, *c* = 10.616 Å, and *V* = 2620 Å³. Elemental anal. Calcd: C, 60.14; H, 5.44; N, 5.04; Cl, 12.74. Obsd: C, 60.29; H, 5.43; N, 5.57.

Li⁺[DDQ]⁻ was prepared in the drybox from LiI (238 mg; 2.01 mmol) and DDQ (269 mg; 1.185 mmol) in acetonitrile. Cooling off the solution to -35 °C for 66 h after filtering afforded microcrystalline product of Li[DDQ]·0.45H₂O composition (154 mg; 0.46 mmol; 38%). Elemental Anal. Calcd: C, 39.70; H, 0.37; N, 11.57; Li, 2.87. Obsd.: C, 39.44; H, 0.31; N, 11.84; Li, 2.88.

Na[HDDQ] was isolated as the monohydrate from a solution of H₂DDQ [(352 mg; 1.538 mmol) 10 mL of EtOH] and NaOH (59.5 mg; 1.488 mmol) [5 mL of 50:50 EtOH:H₂O]. After letting the solution stand for 66 h at ambient temperature yellow needle crystals of NaHDDQ·H₂O composition were isolated by filtration and subsequently vacuum dried at 100 °C overnight (yield 183 mg; 0.68 mmol; 46%). Elemental Anal. Calcd: C, 35.72; H, 1.12; N, 10.41. Obsd.: C, 35.94; H, 1.13; N, 9.97.

Na₂[DDQ] was prepared by the [HDDQ]⁻ procedure except that 2 equiv of NaOH were added to the H₂DDQ. After vacuum drying at 100 °C overnight the composition was determined to be Na₂DDQ·2H₂O. Anal. Calcd: C, 31.10; H, 1.30; N, 9.07. Obsd.: C, 31.20; H, 1.55; N, 8.83.

Results and Discussion

⁵⁷Fe Mössbauer Spectra. Our initial result suggesting that the DDQ species is more appropriately formulated as the *S* = 1/2 [DDQ]⁻ anion in [Fe(C₅Me₅)₂][DDQ] than as the diamagnetic [DDQH]⁻ comes from the observation of a novel fully resolved slow paramagnetic relaxation broadening of the zero-field Mössbauer spectra (Figure 1). Slow paramagnetic relaxation is not common for low-spin iron(III). One of the few and better documented examples¹⁶ is the K₃[Fe(CN)₆] complex isomorphously diluted with the diamagnetic Co^{III} analogue. The combination of dilution (leading to longer spin-spin relaxation times) and very low temperatures (decreasing the rate of spin-lattice relaxation) can ultimately lead to fully resolved magnetic hyperfine splitting of zero-filled Mössbauer spectra. The normal nonobservation of slow paramagnetic relaxation for undiluted low-spin iron(III) compounds is a consequence of the fact that it is a

Kramers ion and its ground state must be at least a spin doublet. There is then the fully allowed nature of transitions (rapid relaxation) between the *m_s* = ±1/2 components of such a doublet. The gradual hyperfine splitting¹⁷ observed in Figure 1 such that *dH_{INT}/dT* is not large is more typical of slow relaxation as opposed to cooperative, extended three-dimensional magnetic order.¹⁸

We find no evidence of slow paramagnetic relaxation-broadening effects in the zero-field Mössbauer spectra of a variety of ferrocenium or decamethylferrocenium salts of simple diamagnetic anions (e.g., [I₃]⁻, [PF₆]⁻, [BF₄]⁻) above 1.7 K. This is also true for the *S* = 0 [C₃(CN)₃]⁻ salt which possesses the same linear chain structure that is observed for the [Fe(C₅Me₅)₂]⁺[DDQ]⁻ salt.¹⁹ We²⁰ and others²¹ have found that external fields, *H*₀, can induce varying degrees of slow paramagnetic relaxation for the case of the [Fe(C₅Me₅)₂]⁺ cation with diamagnetic anions, where the rate of relaxation is related to a complex combination of spin-spin and spin-lattice effects and the magnitude of *H*₀ and is also dependent on the specific type of ferrocenium cations involved. In any event, we believe that the slow relaxation observed for the present system in zero field is consistent with a small Zeeman splitting of the ground-state Kramers doublet of the [Fe(C₅Me₅)₂]⁺ cation by dipolar fields arising from electron spin on the [DDQ]⁻ species in the lattice. This combined with the already large Fe^{III}-Fe^{III} distances²² in the undiluted solid leads to long relaxation times. The shape of the limiting relaxation spectrum (infinitely long relaxation time), Figure 1, is exactly that calculated theoretically by Lang and Oosterhuis²³ for the case of a large positive axial field and an orbital doublet (²E) ground term in the crystal field approximation with the scaling factor for quadrupole interaction very nearly zero owing to electron delocalization and/or a canceling lattice contribution to the electric field gradient. To our knowledge this is the first observation of this limiting form of slow (zero field) relaxation behavior for low-spin Fe^{III}. The preceding ground state is suggested by previous susceptibility²⁴ and spectroscopy²⁵ studies and corresponds to the *a_{1g}*²*e_g*³ [(*d_{xy}*)²(*d_{x²-y²}*)²*d_{xy}*)] configuration. This configuration is expected to lead to both a substantial nonzero field gradient and a quadrupole interaction while nearly zero values are typically observed for various ferrocenium ions. This inconsistency is avoided in molecular orbital treatments²⁶ of the ferrocenium ion which predict essentially zero quadrupole interaction and at the same time allow for electron delocalization.

It is possible that the observed relaxation broadening effects may have as their origin soliton broadening effects.²⁷ To test

(17) The hyperfine splitting at 1.7 K corresponds to a limiting (*T* → 0 K) value of *H_{internal}* of 440 kG for the iron(III) cations in [Fe(C₅Me₅)₂]⁺[DDQ]⁻. This is anomalously large in view of the expected Fermi contact value (*H_F*) of 110 kG/unpaired electron and suggests that a large orbital contribution (*H_L*) to *H_{internal}* is operative. High-field Mössbauer spectra testing this assumption are in progress. These experiments will likely show that *H_{internal}* is positive if it is in fact dominated by *H_L* as opposed to *H_F*.

(18) Cooperative three-dimensional magnetic ordering (ferromagnetism antiferromagnetism, or ferrimagnetism) can also lead to Zeeman splitting of zero-field Mössbauer spectra. However, in these cases the process is usually more sudden, *dH_{INT}/dT* large, and coincident with anomalous behavior in the temperature dependence of the magnetic susceptibility or heat capacity.

(19) Miller, J. S.; Calabrese, J. C.; Chittapeddi, S. R.; Epstein, A. J.; Zhang, J.; Reiff, W. A., manuscript submitted.

(20) Reiff, W. M., unpublished results.

(21) Cohn, M. J.; Timken, M. D.; Hendrickson, D. N. *J. Am. Chem. Soc.* **1984**, *106*, 6683.

(22) The shortest Fe^{III}-Fe^{III} distances along the *a* and *c* axes of the unit cell of [Fe(C₅Me₅)₂]⁺[DDQ]⁻ are all >8.6 Å (ref 7 and private communication with A. H. Reis). In a classic Mössbauer spectroscopy study of slow paramagnetic relaxation of high spin iron(III) compounds, Wignall (Wignall, J. W. G. *J. Chem. Phys.* **1968**, *44*, 2462) has shown that in addition to a slowly relaxing ground-state Kramers doublet, e.g., *m_s* = ±3/2 for quartet Fe^{III} or *m_s* = ±5/2 for sextet, metal-metal separations >7 Å are a necessity for long relaxation times relative to the nuclear Larmor precession frequency leading to resolved hyperfine splittings in zero field.

(23) Lang, G.; Oosterhuis, W. T. *J. Chem. Phys.* **1969**, *51*, 3608.

(24) Hendrickson, D. N.; Sohn, Y. S.; Gray, H. B. *Inorg. Chem.* **1971**, *10*, 1559.

(25) Duggan, D. M.; Hendrickson, D. N. *Inorg. Chem.* **1975**, *14*, 955.

(26) Collins, R. L. *J. Chem. Phys.* **1965**, *42*, 1072.

(27) Thiel, R. D.; DeGraaf, H.; De Jongh, L. J. *Phys. Rev. Lett.* **1981**, *47*, 1415. De Jongh, L. J., *J. Appl. Phys.* **1982**, *53*, 8018.

(13) Pulay, P. In *Applications of Electronic Structure Theory*; Schaefer, H. F., III, Ed.; Plenum Press: New York, 1977; p 153.

(14) Pasimeni, L.; Brustolon, M.; Zanonato, P. L.; Corvaja, C. *Chem. Phys.* **1980**, *51*, 381-387.

(15) Zanotti, G.; Del Pra, A.; Bozio, R. *Acta Crystallogr.* **1982**, *B38*, 1225-1229.

(16) Oosterhuis, W. T.; Lang, G. *Phys. Rev.* **1969**, *178*, 439.

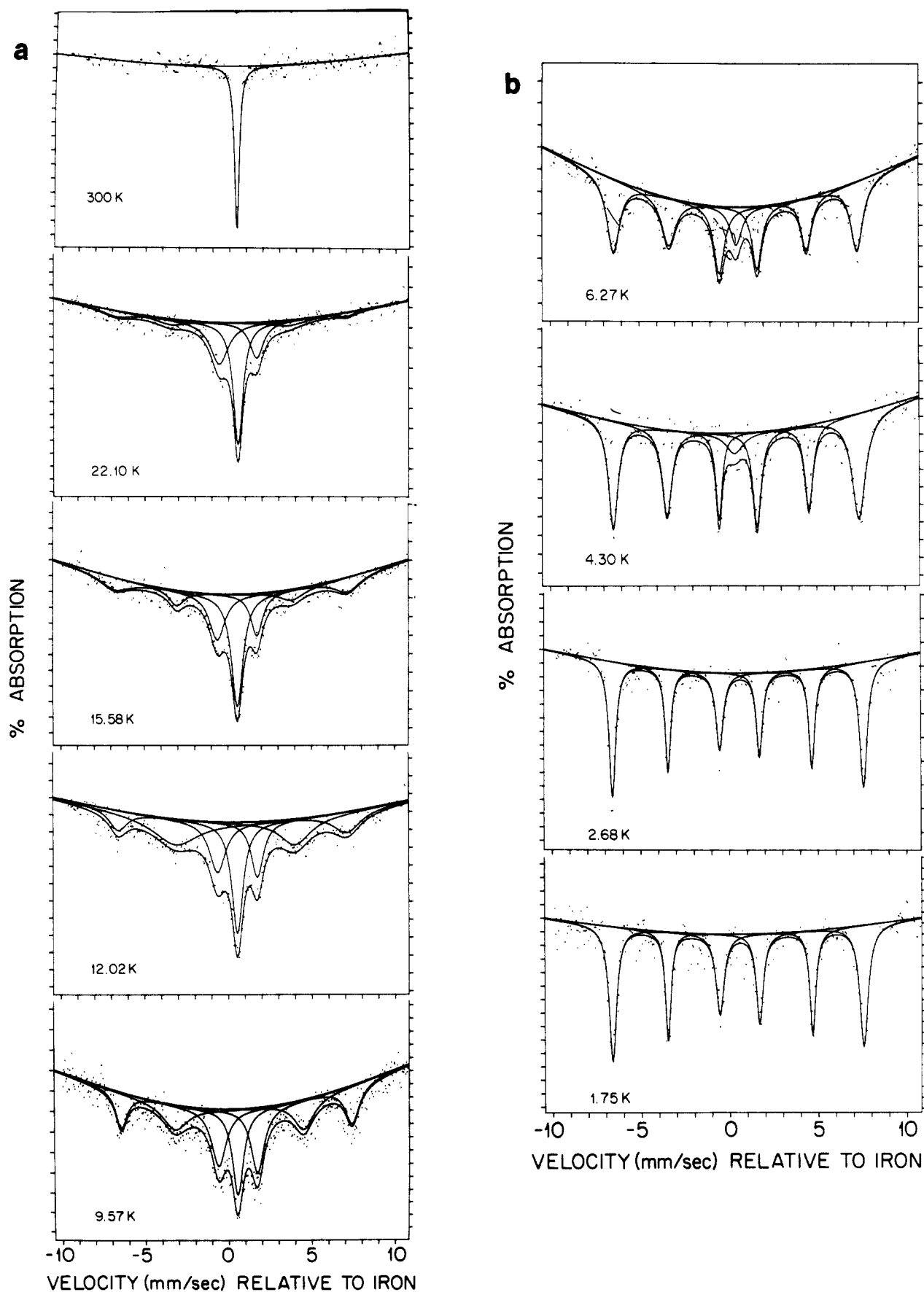


Figure 1. Zero-field Mössbauer spectra of $[\text{Fe}(\text{C}_5\text{Me}_5)_2]^+\cdot[\text{DDQ}]^{\bullet-}$: (a) 300–9.57 K, (b) 6.27–1.75 K.

this possibility careful measurements of the Mössbauer spectral line widths immediately above and below the true magnetic ordering temperature as well as the precise determination of the critical transition temperature (e.g., by heat capacity) are a ne-

cessity. These experiments are in progress.

Electron Spin Resonance. Dilute solutions of $[\text{Co}(\text{C}_5\text{H}_5)_2]\text{[DDQ]}$ and $[\text{Co}(\text{C}_5\text{Me}_5)_2]\text{[DDQ]}$ in various solvents (e.g., acetonitrile, 10:1 THF/HMPA, glyme) display an intense ESR

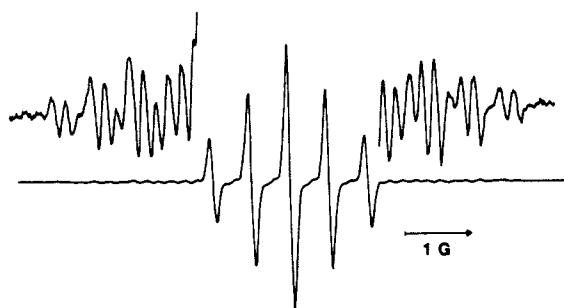


Figure 2. ESR spectrum of $[\text{Co}(\text{C}_5\text{H}_5)_2][\text{DDQ}]$ in THF/HMPA (10:1) at 0 °C.

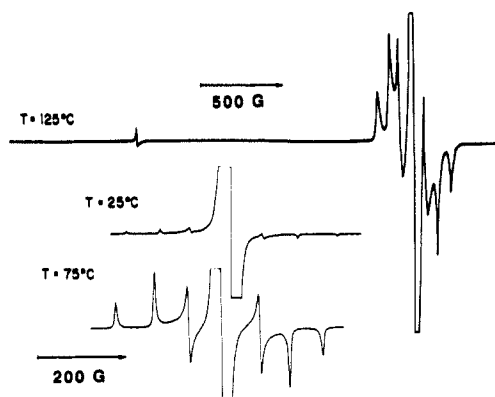


Figure 3. ESR spectra of a finely powdered sample of $[\text{Co}(\text{C}_5\text{H}_5)_2][\text{DDQ}]$ at 125, 75, and 25 °C. A wider scan was used at 125 °C to show the half-field $\Delta M = 2$ triplet-state transition ($g = 4.0192$).

spectrum of the $[\text{DDQ}]^{\cdot-}$ radical anion identical with that observed for $[\text{Et}_4\text{N}]^+[\text{DDQ}]^{\cdot-}$ in the same solvents or with that obtained in the reaction of DDQ with sodium naphthalide in THF.²⁹ Optimum resolution was obtained in 10:1 THF:HMPA at 0 °C (Figure 2). The spectrum consists of a quintet appropriate for a weak hyperfine interaction of the unpaired electron with two equivalent ^{14}N nuclei (0.59 G; $g = 2.00517$). At high gain ^{13}C satellite lines can be easily detected. They reveal hyperfine interactions with three of the four types of ^{13}C atoms of the $[\text{DDQ}]^{\cdot-}$ radical anion (4.72, 4.31, and 2.78 G), the fourth having a splitting which is too small to be seen. ESR spectra of acetonitrile solutions of $[\text{Co}(\text{C}_5\text{H}_5)_2][\text{DDQ}]$ and of $[\text{Co}(\text{C}_5\text{Me}_5)_2][\text{DDQ}]$ of known concentrations were compared by double integration under strictly comparable conditions against those of the (4-hydroxy-2,2,6,6-tetramethylpiperidyl)oxy radical standard. This comparison established that the concentrations of the $[\text{DDQ}]^{\cdot-}$ radical anion in solution were within experimental error with those expected for a 1:1 radical ion salt.

Finely divided powder samples of $[\text{Co}(\text{C}_5\text{H}_5)_2][\text{DDQ}]$ at room temperature and low gains display a single ESR line ($\Delta H = 5$ G) with a g factor ($g = 2.0052$) indistinguishable from that of the $[\text{DDQ}]^{\cdot-}$ radical anion in solution. Comparisons by double integrations of the intensity of this line for weighed samples against the intensities for weighed samples of DPPH (diphenylpicrylhydrazyl) established that the intensity of this line is less than 1% of the intensity expected if all $[\text{DDQ}]^{\cdot-}$ radical anions in the samples contributed to the signal. At higher gains, however, an additional spectrum characteristic of randomly oriented triplet states can be seen³⁰ (Figure 3). The intensity of this signal grows as the temperature increases up to 180 °C, where irreversible damage to the sample begins. Thus, only a small number of $[\text{DDQ}]^{\cdot-}$ radical anions contribute to the doublet state ESR signal and to the magnetic susceptibility, and there exists a low-lying

Table I. Zero-Field Splitting Parameters and Singlet-Triplet Separation Energies for $[\text{DDQ}]^{\cdot-}$ Salts

complex	J (eV)	$ D $ (G)	$ E $ (G)
$[\text{Co}(\text{C}_5\text{H}_5)_2][\text{DDQ}]^a$	0.25	232 ^b	24 ^c
$[\text{Co}(\text{C}_5\text{H}_5)_2][\text{DDQ}]^d$	0.25	229	24
$[(\text{CH}_3)_4\text{N}][\text{DDQ}]^e$	0.19	209	21
$[(\text{C}_2\text{H}_5)_4\text{N}][\text{DDQ}]^e$	0.30	227	22
$[(\text{C}_3\text{H}_7)_4\text{N}][\text{DDQ}]^e$	0.27	231	26
$[(\text{C}_4\text{H}_9)_4\text{N}][\text{DDQ}]^e$	0.21	198	19

^a 50 °C. ^b 0.0217 cm^{-1} . ^c 0.0022 cm^{-1} . ^d 100 °C. ^e From ref 31.

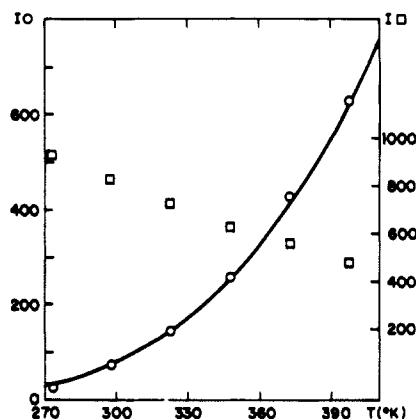


Figure 4. Experimental and calculated temperature dependencies of the integrated intensity of the $\Delta M = 2$ absorption of $[\text{Co}(\text{C}_5\text{H}_5)_2][\text{DDQ}]$ (circles) and temperature dependence of the integrated intensity of the $g = 2.00$ absorption of $[\text{Co}(\text{C}_5\text{Me}_5)_2][\text{DDQ}]$ (squares) in arbitrary units.

triplet state. This is consistent with a solid-state structure consisting of $[\text{DDQ}]_2^{2-}$ dimers having a singlet ground state with a thermally accessible excited triplet state which can be increasingly populated as the temperature is raised. This situation has been found in a number of radical ion salts which have in their crystal structures linear chains of planar radical ions stacked in a tilted face-to-face arrangement with strong alternation in the distances between the molecular planes. In effect, one has a stacking of dimeric units within which the unpaired electrons are coupled by exchange interactions. The excited triplet states of such units have been shown to be mobile triplet excitons. The $[\text{R}_4\text{N}]^+[\text{DDQ}]^{\cdot-}$ ($\text{R} = \text{Me}, \text{Et}, \text{Pr}, \text{Bu}$) radical ion salts which have been studied in single crystals also display such a behavior.^{14,31} Indeed, in the $[(\text{C}_2\text{H}_5)_4\text{N}]^+[\text{DDQ}]^{\cdot-}$ radical ion salt the periodic dimerization in the anion columns is particularly pronounced compared with other radical ion salts (inter- and intradimer spacings: 3.626 and 2.906 Å), suggesting that the attractive interaction between permanent dipole moments of the $[\text{DDQ}]^{\cdot-}$ anions may contribute to the stabilization of dimeric structures in $[\text{DDQ}]^{\cdot-}$ radical ion salts.³²

The zero-field splitting parameters D and E describing the dipole-dipole interaction of the triplet-state electrons were extracted from the triplet-state powder spectra of $[\text{Co}(\text{C}_5\text{H}_5)_2][\text{DDQ}]$ with equations³⁰ 1–3, where ΔH_z is the separation in Gauss

$$\Delta H_z = 2D \quad (1)$$

$$\Delta H_y = D + 3E \quad (2)$$

$$\Delta H_x = D - 3E \quad (3)$$

between the outermost pair of absorptions, ΔH_y is the separation between the next pair of absorptions, and ΔH_x is the separation between the innermost pair of derivative-like features of the triplet-state powder spectrum (Figure 3). The values of the D and E parameters at 50 and 100 °C are compared in Table I with the values for other $[\text{DDQ}]^{\cdot-}$ radical ion salts. It is seen that

(28) Corvaja, C.; Pasimeni, L.; Brustolon, M. *Chem. Phys.* **1976**, *14*, 177.

(29) Prepared in situ from $\text{Na}^+[\text{C}_{10}\text{H}_8]^{\cdot-}$ in THF. The reaction is chemiluminescent where probably $[\text{C}_{10}\text{H}_8]^{\cdot-} \rightarrow [\text{C}_{10}\text{H}_8]^* + e^- \rightarrow \text{C}_{10}\text{H}_8 + h\nu$.

(30) Wasserman, E.; Snyder, L. C.; Yager, W. A. *J. Chem. Phys.* **1964**, *41*, 1763.

(31) Gordon, D.; Hove, N. J. *J. Chem. Phys.* **1973**, *59*, 3419.

(32) (a) Zanotti, G.; Bardi, R.; Del Pra, A. *Acta Crystallogr., Sect. B* **1980**, *36*, 168. (b) Herbststein, F. H.; Kapon, M.; Rjonjew, G.; Rabinovich, D. *Ibid.* **1978**, *34*, 476. (c) Bernstein, J.; Regev, H.; Herbststein, F. H. *Ibid.* **1977**, *33*, 1716.

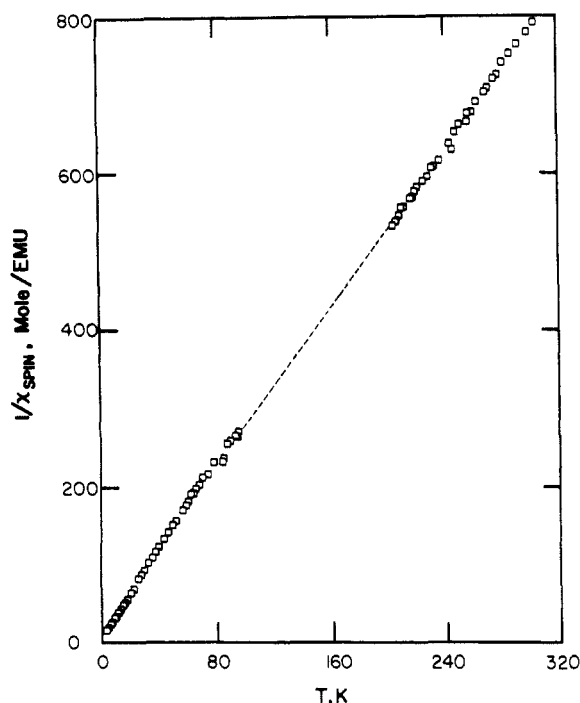


Figure 5. Reciprocal magnetic susceptibility of $[\text{Co}(\text{C}_5\text{Me}_5)_2]^+[\text{DDQ}]^{\bullet-}$ as a function of temperature. The 300 K value for the reciprocal susceptibility of $[\text{Co}(\text{C}_5\text{H}_5)_2][\text{DDQ}]$ is $\sim 1 \times 10^5$ mol/emu. The data between ~ 100 and 200 K, as indicated by a dashed line, are absent. The measured susceptibility in this range had larger than usual errors due to the lack of thermal equilibrium between the sample and temperature sensor.

$[\text{Co}(\text{C}_5\text{H}_5)_2][\text{DDQ}]$ is quite similar to the organic $[\text{DDQ}]^{\bullet-}$ salts with respect to the triplet exciton behavior. Above 150°C the triplet state powder spectrum begins to broaden dramatically, indicating the onset of the coalescence of the triplet-state fine structure into a single peak by fast spin exchange during collisions of triplet excitons.³³

The temperature dependence of the integrated intensity, I , of the $\Delta M = 2$ absorption for $[\text{Co}(\text{C}_5\text{H}_5)_2][\text{DDQ}]$ is shown in Figure 4. The singlet-triplet separation energy, J , can be determined by fitting eq 4 to these points.³⁴

$$I \propto [T \exp(J/kT) + 3]^{-1} \quad (4)$$

An initial value of J can be obtained from $I \propto [\exp(-J/kT)]/T$ which is valid for sufficiently large values of J/kT . A plot of $\ln(I/T)$ vs. T^{-1} yields a straight line of slope $-J/k$.³⁵ The calculated curve of Figure 4 corresponds to $J = 0.25$ eV (5.7 kcal/mol). This value is comparable to that reported for $\text{K}[\text{TCNQ}]$ ³⁶ but is larger than those reported for most other radical anion salts.^{36,37} It also compares well with those found for other $[\text{DDQ}]^{\bullet-}$ radical ion salts (Table I) reflecting the particular stabilization of $[\text{DDQ}]^{\bullet-}$ dimeric units in these salts.

Powder samples of $[\text{Co}(\text{C}_5\text{Me}_5)_2][\text{DDQ}]$ also display a single ESR absorption similar to that of $[\text{Co}(\text{C}_5\text{H}_5)_2][\text{DDQ}]$ except that it is strikingly more intense. Intensity, I , comparisons against DPPH indicate that within experimental error all $[\text{DDQ}]^{\bullet-}$ radical anions of the sample contribute to the signal. Furthermore, the temperature dependence of this absorption (Figure 4) has a slope conforming to the Curie law ($dI/dT < 0$) as expected for a doublet state. This is consistent with the structure, i.e., it is isomorphous to $[\text{Fe}(\text{C}_5\text{Me}_5)_2][\text{DDQ}]$ ⁷ which possesses isolated $[\text{DDQ}]^{\bullet-}$ groups which are too far apart to form $S = 0$ dimers.

Magnetic Susceptibility. Room temperature static magnetic

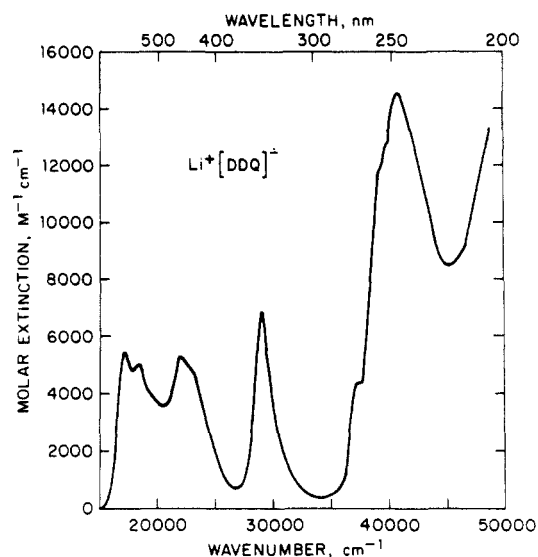


Figure 6. Absorption spectra of $[\text{Li}][\text{DDQ}]$ (1.36×10^{-3} M) in acetonitrile.

susceptibility is in agreement with the ESR results for $[\text{Co}(\text{C}_5\text{H}_5)_2][\text{DDQ}]$. After correction for the core diamagnetism the observed spin susceptibility corresponds to $< 0.01 S = 1/2$ Curie spin per formula unit. This confirms Hendrickson and co-workers³⁴ result that $[\text{Co}(\text{C}_5\text{H}_5)_2][\text{DDQ}]$ solid is essentially diamagnetic and spin impurities can account for the observed susceptibility and ESR signal. In contrast to the low susceptibility observed for solid samples of $[\text{Co}(\text{C}_5\text{H}_5)_2][\text{DDQ}]$, $[\text{Co}(\text{C}_5\text{Me}_5)_2][\text{DDQ}]$ as a solid exhibits magnetic susceptibility (via ESR and Faraday techniques) consistent with one unpaired electron per DDQ. The temperature dependence of the susceptibility obeys the Curie-Weiss law, $C/(T + \theta)$ with $\theta = 1 \pm 1$ K (Figure 5). This is in agreement with a linear chain structure of alternating $[\text{DDQ}]^{\bullet-}$ radicals and diamagnetic $[\text{Co}(\text{C}_5\text{Me}_5)_2]^+$. The absence of strong exchange coupling among $[\text{DDQ}]^{\bullet-}$ spins parallels the absence of strong exchange coupling between $[\text{Fe}(\text{C}_5\text{Me}_5)_2]^+$ spins in salts with diamagnetic anions and similar crystal structure (e.g., $[\text{Fe}(\text{C}_5\text{Me}_5)_2]^+[\text{C}_3(\text{CN})_3]^-$). The low temperature and the magnetic field dependence of the magnetization of a single crystal of $[\text{Fe}(\text{C}_5\text{Me}_5)_2]^+[\text{DDQ}]^{\bullet-}$ were remeasured for magnetic fields parallel to the chain axis. The results agree with our previously published study, with both the magnetic field behavior and saturation moment in accord with spin $1/2$ with $g \sim 4$ on the $[\text{Fe}(\text{C}_5\text{Me}_5)_2]^+$ and the absence of a contribution due to the spin $1/2$ expected from the $[\text{DDQ}]^{\bullet-}$. See ref 7 for a detailed discussion for this assignment.

Infrared Spectra. The infrared spectra of $[\text{Co}(\text{C}_5\text{H}_5)_2][\text{DDQ}]$ and $[\text{Fe}(\text{C}_5\text{Me}_5)_2][\text{DDQ}]$ were taken and compared with those of DDQ, $[\text{DDQ}]^{\bullet-}$, $[\text{DDQH}]^-$, $[\text{DDQ}]^{2-}$, and DDQH_2 . In Table II are listed the key infrared absorptions for the DDQ family of compounds. Note that $[\text{DDQH}]^-$ exhibits a characteristic ν_{OH} absorption at 3553 (sharp, m). These absorptions are not present in the infrared spectra obtained for $[\text{Co}(\text{C}_5\text{H}_5)_2][\text{DDQ}]$ [$3110 (\nu_{\text{C-H}}, \text{w})$, $2220 (\nu_{\text{C=N}}, \text{m})$, 1575 , 1520 cm^{-1}] and $[\text{Fe}(\text{C}_5\text{Me}_5)_2][\text{DDQ}]$ [3100 , $2960 (\nu_{\text{C-H}}, \text{w})$, $2200 (\nu_{\text{C=N}}, \text{m})$, 1540 , 1515 cm^{-1}]. The lack of the ν_{OH} absorption provides further evidence against the presence of $[\text{DDQH}]^-$ anion for these compounds.

Electronic Absorption Spectra. The electronic absorption spectra of DDQ, $[\text{DDQ}]^{\bullet-}$, $[\text{DDQH}]^-$, DDQH_2 , and $[\text{DDQ}]^{2-}$ are reported in Table III. The $[\text{DDQ}]^{\bullet-}$ radical anion recorded both as the $[\text{Et}_4\text{N}]^+$ and Li^+ salts is the only species which has appreciable absorption in the visible portion of the spectra (Figure 6). The multitude of characteristic absorptions clearly characterizes $[\text{DDQ}]^{\bullet-}$ as being distinct from $[\text{DDQH}]^-$. The identical $[\text{DDQ}]^{\bullet-}$ spectrum is observed when $[\text{DDQ}]^{\bullet-}$ is formed electrochemically or chemically from the reaction of DDQ and $\text{Na}^+[\text{C}_{10}\text{H}_8]^{\bullet-}$. Opening the cuvette to air for extended periods of time (ca. 1 day) does not change the spectra. Addition of a drop of water to the $[\text{DDQ}]^{\bullet-}$ cuvette does effect a color change

(33) Soos, Z. G. *J. Chem. Phys.* **1967**, *46*, 4284.

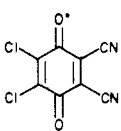
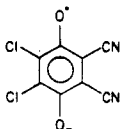
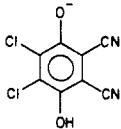
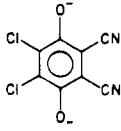
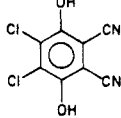
(34) Chesnut, D. B.; Phillips, W. D. *J. Chem. Phys.* **1961**, *35*, 1002.

(35) Chesnut, D. B.; Arthur, P., Jr. *J. Chem. Phys.* **1962**, *36*, 2969.

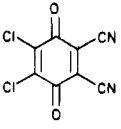
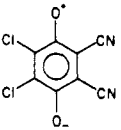
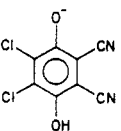
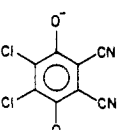
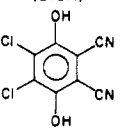
(36) Jones, M. T.; Jansen, S.; Roble, J.; Ashwell, G. *J. Mol. Cryst. Liq. Cryst.* **1985**, *120*, 111-114.

(37) McGlynn, S. P.; Azumi, T.; Kinoshita, M. *Molecular Spectroscopy of the Triplet State*; Prentice Hall, Inc.: New York, 1969; p 394.

Table II. Characteristic Infrared Absorptions for Model DDQ Compounds^a

	ν_{OH}	ν_{CN}	$\nu_{\text{C=O}}$	$\nu_{\text{C=C}}$	$\nu_{\text{aromatic C=C}}$
		2234 w 2246 w	1691 s 1701 s	1550 w	
		2217 s			1580 s
	3553 m	2243 s		1675 s	1460 s
		2187 m 2200 s		1618 w	1457 s
	3295 br, s	2257 2269			1575 m 1465 s

^a Powder. ^b [NEt₄]⁺ salt. ^c Na⁺ salt. s = strong; w = weak; br = broad; d = doublet.**Table III.** Characteristic Electronic Absorptions for Model DDQ Compounds

compound (solvent)	λ_{max} , nm	λ_{max} , cm ⁻¹	ϵ , M ⁻¹ cm ⁻¹
	372 280 270 226 216 209	26 850 35 700 37 000 44 250 46 300 47 850	870 12 300 11 500 14 600 15 300 15 700
(MeCN)			
	588 547 508 456 432 347 323 sh 270 257 sh 247	17 000 18 300 19 700 21 900 23 150 28 800 30 950 37 000 38 900 40 500	6 300 5 775 4 350 6 050 5 275 7 800 1 890 4 925 12 900 16 225
(MeCN)			
	397 249 205	25 200 40 150 42 800	10 050 24 200 23 850
(EtOH)			
	452 398 248 205	22 125 25 125 40 325 48 800	9 100 22 100 23 400 700
(EtOH)			
	420 350 260 230 217	23 800 28 575 38 450 43 475 46 100	200 8 700 8 200 23 000 39 800
(EtOH)			

over an extended period of time; however, no change is immediately evident (~ 0.25 h).**Table IV.** Geometry Parameters for DDQ and [DDQ]^{•-}^a

	DDQ		[DDQ] ^{•-}	
parameter	calcd	exptl ²⁸	calcd	exptl ^{8,29}
$r(\text{C}_1-\text{C}_1')$	1.334	1.341	1.386	1.385
$r(\text{C}_1-\text{C}_2)$	1.522	1.496	1.445	1.444
$r(\text{C}_2-\text{C}_3)$	1.520	1.482	1.481	1.459
$r(\text{C}_3-\text{C}_3')$	1.325	1.344	1.340	1.366
$r(\text{C}_1-\text{C}_4)$	1.458	1.455	1.454	1.434
$r(\text{C}_4-\text{N})$	1.158	1.135	1.163	1.120
$r(\text{C}_2-\text{O})$	1.222	1.209	1.310	1.246
$r(\text{C}_3-\text{Cl})$	1.768	1.715	1.789	1.724
$\theta(\text{C}_1-\text{C}_1-\text{C}_2)$	122.1	121.6	122.5	122.7
$\theta(\text{C}_1-\text{C}_2-\text{C}_3)$	115.6	116.7	114.8	114.6
$\theta(\text{C}_2-\text{C}_3-\text{C}_3')$	122.3	121.8	122.7	122.2
$\theta(\text{C}_1-\text{C}_1-\text{C}_4)$	121.8	122.2	120.5	120.3
$\theta(\text{C}_2-\text{C}_1-\text{C}_4)$	116.2	116.2	116.9	117.0
$\theta(\text{C}_1-\text{C}_4-\text{C}_5)$	180.0	178.2	179.6	178.4
$\theta(\text{C}_1-\text{C}_2-\text{O})$	121.9	120.2	123.7	122.5
$\theta(\text{C}_3-\text{C}_2-\text{O})$	122.5	123.1	121.5	123.0
$\theta(\text{C}_2-\text{C}_3-\text{Cl})$	114.7	115.8	115.7	115.4
$\theta(\text{C}_3-\text{C}_3-\text{Cl})$	123.0	122.4	121.7	120.8

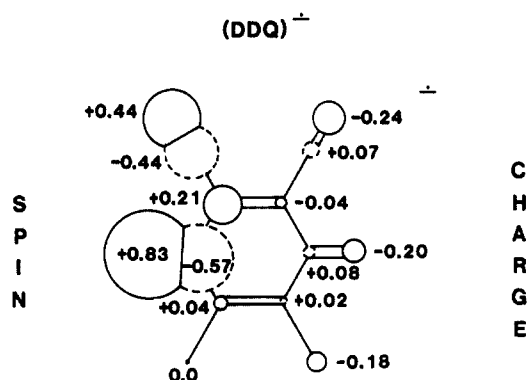
^a Bond distances in Å. Bond angles in deg.

The electronic absorption spectra of [Co(C₅H₅)₂][DDQ], [Fe(C₅Me₅)₂][DDQ], [Co(C₅H₅)₂][PF₆], and [Fe(C₅Me₅)₂][BF₄] were also recorded. All of the spectral features noted for the DDQ salts of these metallocenium cations can be assigned, and clearly evident is the quantitative presence of [DDQ]^{•-}.

Molecular Orbital Calculations. The atom labeling and geometric parameters for DDQ and [DDQ]^{•-} are given in Table IV where they are compared with averaged sets of literature values.^{15,32} The agreement with most of the parameters is excellent, considering the quality of the basis set. For DDQ the only significant error in the geometry is found for the C-Cl bond length

Table V. Charges and Spin Populations^a for DDQ and [DDQ]^{•-}

atom ^a	Charge		tot spin pop [DDQ] ^{•-}	valence s orbital spin pop ^b [DDQ] ^{•-}	valence p _z orbital spin pop ^b [DDQ] ^{•-}
	q(DDQ)	q([DDQ] ^{•-})			
C ₁	+0.03	-0.04	+0.21	0.031	0.13
C ₂	+0.21	+0.08	-0.57	-0.071	-0.41
C ₃	+0.04	+0.02	+0.04	0.011	0.01
C ₄	+0.08	+0.07	-0.44	-0.055	-0.18
N	-0.14	-0.24	+0.44	0.021	0.21
O	-0.15	-0.20	+0.83	0.022	0.75
Cl	-0.07	-0.18	0.00	0.000	0.00

^a See Table IV for atom labeling. ^b Populations in units of electrons.**Figure 7.** Calculated charge (right-hand side) and spin (left-hand side) distributions for [DDQ]^{•-}.

which the theory predicts to be too long by 0.053 Å. This type of error is typical when the STO-3G basis set is used for compounds with bonds to second-row atoms.³⁸ Other relevant differences are that the theory predicts the C=O and C≡N bonds to be slightly longer than the experimental values.

The calculated structure of [DDQ]^{•-} shows somewhat larger deviations from the averaged experimental structure. As expected from DDQ, the calculated C-Cl bond is too long; however, it does show the increase expected from experiment. The C≡N bond is predicted to lengthen slightly in [DDQ]^{•-} as compared to DDQ which is opposite to the experimental result. Whether this is an artifact of the calculations or a problem in the crystal structure determination requires further study. We note that the studies of Zanotti et al.^{14,32a} on DDQ and [DDQ]^{•-} do suggest that little change for the CN bond in [DDQ]^{•-} should be found as compared to DDQ. The other large difference between the experimental and calculated structures is the value for *r*(C=O). Both experiment and theory predict that *r*(CO) should increase in going from DDQ to [DDQ]^{•-}. The experimental increase is 0.035 Å as compared to the calculated increase of 0.088 Å. Thus, the calculation exaggerates the change in the C=O bond length. This probably arises from the localization of the excess electron spin (excess charge) on the oxygen which would require a significantly larger basis set (possibly including diffuse functions) to get good agreement with experiment.

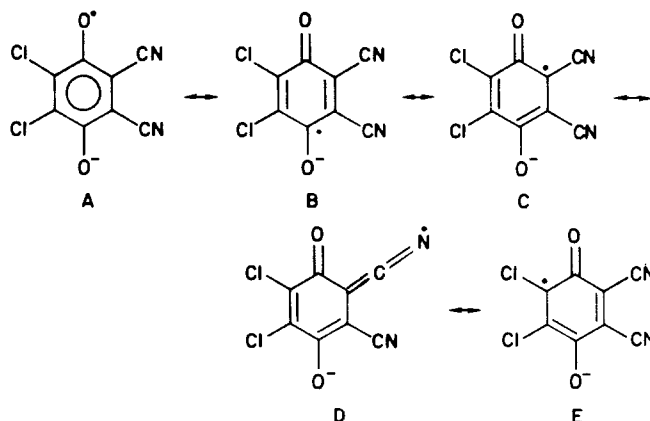
The charge and spin distributions are given in Table V and Figure 7. The charge distributions for DDQ are as expected; the carbons are all positive and the N, O, and Cl are negative. The most polar bond is the CO bond. The calculated value for the dipole moment is 1.46 D. Addition of an electron to form [DDQ]^{•-} increases the negative charge on the N, O, and Cl. The charges on all carbons except C₄ become significantly less positive with C₁ even having a negative charge. The most polar bond is now with the CN bond instead of the C=O bond.

The atomic spin populations in [DDQ]^{•-} show some interesting trends. The spin populations are defined as the difference between the Mulliken populations for the α and β electrons with there being one excess α electron. (Positive spin implies an excess population of α electrons.) The total spin populations show that there are

Table VI. Highest Occupied and Lowest Unoccupied Molecular Orbital Energies and Symmetries for DDQ

occupied		virtual	
energy, eV	symmetry	energy, eV	symmetry
9.60	b ₁ (π)	-1.63	a ₂ (π*)
10.05	b ₁ (π)	-4.35	a ₂ (π*)
10.99	b ₂ (σ)	-6.57	b ₁ (π*)
11.83	b ₂ (σ)	-6.75	a ₁ (σ*)
12.41	a ₂ (π)		
12.43	a ₁ (σ)		

significant positive spin (excess α) at C₁, N, and O and significant amounts of negative spin (excess β) at C₂ and C₄. This is consistent with simple models of spin polarization.³⁹ The results show that the excess α spin is localized predominantly in the C=O and C≡N bonds. The results can be examined in terms of the resonance structures given below (each resonance structure appears twice). A is the dominant resonance structure followed by D and



C. Structures B and E do not make major contributions. The large negative spin population at C₂ is thus mainly due to the polarization of the spin due to the excess spin at oxygen. The large negative spin at C₄ is consistent with the absence of a resonance structure placing spin at this carbon.

We also report the spin populations in the 2s and 2p_z orbitals in Table V. The calculation shows that the excess spin is largely localized in the out-of-plane p_z orbitals for C₁ and O. This would be expected since the LUMO for DDQ is an out-of-plane p_z orbital. The spin in the CN bonds also has an in-plane p_z component consistent with the behavior of other cyano-substituted radical anions.¹⁹ The ESR behavior is governed by the interaction of the spins in the s orbitals with the nuclear spins since these are the only orbitals with a nonvanishing component at the nucleus. On the basis of these values we would assign the largest ¹³C hyperfine splitting to be at C₂ with the next largest at C₄. The smaller hyperfine constant would be at C₁. We would also assign negative values to the coupling constants at C₂ and C₄ and a positive value at C₁. Finally, the ¹³C hyperfine interaction at C₃ should be very small. These results are similar to those of Corvaja

(38) Hendewerk, M. L.; Frey, R.; Dixon, D. A. *J. Phys. Chem.* **1983**, *87*, 2026.(39) Carrington, A.; McLachlan, A. D. *Introduction to Magnetic Resonance*; Harper and Row: New York, 1967.

et al.,²⁸ who performed a McLachlan calculation⁴⁰ of the spin density distribution. The only difference is that they would predict the hyperfine interaction to be larger at C₄ than at C₂.

The molecular orbitals for DDQ (Table VI) and [DDQ]^{•-} can be used as an aid in interpreting the electronic absorption spectrum observed for [DDQ]^{•-}. The HOMO and NHOMO of DDQ are π -orbitals (b₁ symmetry) and are located at 9.60 and 10.05 eV, respectively. The LUMO and the next two UMO's are also π -orbitals with symmetry labels of a₂, a₂, and b₁. For DDQ the transitions among the π -orbitals are all symmetry allowed.

Addition of an electron to DDQ to give [DDQ]^{•-} should give a ²A₂ state based on the DDQ orbitals; this is confirmed by the calculations on [DDQ]^{•-}. For [DDQ]^{•-} there are two types of transitions that can occur due to the presence of the singly occupied molecular orbital (SOMO). We define a set of internal transitions which involve excitation from the doubly occupied orbitals to the SOMO and external transitions as excitations from the occupied orbitals including the SOMO to the unoccupied (virtual) orbitals. Addition of an electron to DDQ is an exothermic process, i.e., DDQ has a positive electron affinity.⁴¹ This leads to a stabilization of the orbital to which the electron is added and a destabilization of the other occupied orbitals due to the presence of the negative charge. The HOMO-LUMO energy gap in DDQ becomes the SOMO-NHOMO in [DDQ]^{•-}. The difference in the SOMO-NHOMO energy in [DDQ]^{•-} will be less than that of the HOMO-LUMO energy difference in DDQ. Thus, the HOMO-LUMO transition in DDQ is now an "internal" transition for [DDQ]^{•-} and should be significantly shifted to the red as compared to DDQ. Such behavior has previously been found for TCNQ and [TCNQ]^{•-}.⁴² As a consequence of the stabilization of the SOMO in [DDQ]^{•-}, the other UMO's will be destabilized and this energy difference between the SOMO and LUMO should increase. We thus assign the observed transition in the range of 18000–25000 cm⁻¹ to be the first internal transition ²A₂ ← ²B₁ which is allowed. We qualitatively assign the structure in the band as being due to a vibrational progression with a frequency of ~1300 cm⁻¹. Since the HOMO and NHOMO are close in energy in DDQ, it is quite possible that the band consists of two overlapping internal transitions adding to the complexity. The sharp pronounced transition at 28800 cm⁻¹ could be due to the SOMO → LUMO transition, but this assignment is tentative at best. The transitions below 33000 cm⁻¹ are probably due to SOMO → LUMO transitions and are in the range observed for other cyano-substituted carbanions.⁴³

(40) McLachlan, A. D. *Mol. Phys.* **1960**, 3, 244.

(41) The electron affinity obtained by polarographic half-wave potentials is 3.0 eV (Chen, E. C. M.; Wentworth, W. E. *J. Chem. Phys.* **1975**, 63, 3183–3191).

(42) Zanon, I.; Pecile, C. *J. Phys. Chem.* **1983**, 87, 3657.

Conclusion

Our previous report that [Fe(C₅Me₅)₂][DDQ] contains the [DDQH]⁻ diamagnetic anion, although consistent with prevailing wisdom, was erroneous. On the basis of the collective evidence provided by solution electronic and vibrational spectra as well as ESR data, it is clear that the anion is S = 1/2 [DDQ]^{•-}. The structure of the isolated [DDQ]^{•-} is that which was reported in our previous work and is consistent with the MO calculation.⁷

The line of logic that leads to the postulation of [DDQH]⁻ followed from the work of Hendrickson et al.³ on [Co(C₅H₅)₂][DDQ]. On the basis of its diamagnetic behavior in the solid (which we confirm) they formulated [DDQH]⁻. We have extended our study to include its solution behavior where we observe ESR, electronic, and vibrational spectra associated with [DDQ]^{•-}. We suggest that deviations between the solution and solid state behavior are due to dimerization of [DDQ]^{•-} to form diamagnetic [DDQ]₂²⁻ in the solid. Structural evidence for [DDQ]₂²⁻ exists. It is seen in the [N(C₂H₅)₄]⁺¹⁵ and tetrathiafulvalenium⁺⁴⁴ salts where intradimer separations of 2.906 and 2.97 Å, respectively, are present. Thus, we propose that dimerization of [DDQ]^{•-} either as isolated dimers or chains of dimers accounts for the diamagnetism in [Co(C₅H₅)₂][DDQ]^{•-}. In the [Co(C₅Me₅)₂][DDQ]^{•-} a full spin is observed by ESR and Faraday techniques. This is in accord with an isolated [DDQ]^{•-} ion present in the structure.

Given the reformulation of [Fe(C₅Me₅)₂][DDQ] to consist of S = 1/2 cations and anions in the solid we are in the process of a reinterpretation of the magnetic susceptibility. We suggest that other ferrocenium and biferrocenium salts of DDQ postulated to possess diamagnetic [DDQH]⁻ be reinvestigated.

Acknowledgment. We thank D. B. Chase, C. G. Chetkowski, F. Davidson, W. R. Bachman, R. L. Harlow, G. Hyatt, D. Jones, R. Richardson (Du Pont CR&D), R. Bigelow (Xerox), and J. F. Lomax and T. J. Marks (Northwestern) for their technical assistance and helpful suggestions. W. M. Reiff and J. H. Zhang are pleased to acknowledge the continued support of the NSF-DMR solid state chemistry program currently under Grant No. 8313710.

Registry No. [Et₄N]⁺[DDQ]^{•-}, 50915-73-6; [Et₄N]⁺I⁻, 68-05-3; DDQ, 84-58-2; [Co(C₅Me₅)₂]⁺[DDQ]^{•-}, 102261-47-2; Co(C₅Me₅)₂, 74507-62-3; Li⁺[DDQ]^{•-}, 93030-13-8; LiI, 10377-51-2; Na[HDDQ], 102261-49-4; Na₂[DDQ], 102283-20-5; H₂DDQ, 4640-41-9; [Fe(C₅Me₅)₂]⁺[DDQ]^{•-}, 102261-48-3; [Co(C₅H₅)₂]⁺[DDQ]^{•-}, 12288-03-8; [DDQ]^{•-}, 34505-22-1; [DDQH]⁻, 46257-45-8; [DDQ]₂²⁻, 59637-65-9.

(43) Dixon, D. A.; Calabrese, J. C.; Miller, J. S. *J. Am. Chem. Soc.* **1986**, 108, 2582–2588.

(44) Mayerle, J. J.; Torrance, J. B. *Bull. Chem. Soc. Jpn.* **1981**, 54, 3170–3172.